Development of near- and mid-infrared imaging spectrometers for the Martian moon's sample return mission and next generation space projects

*Takeshi Sakanoi[1], Takahiro Iwata[2], Tomoki Nakamura[4], Yasumasa Kasaba[4], Makoto Taguchi[5], Hiromu Nakagawa[4], Masato Kagitani[1], Atsushi Yamazaki[2], Shohei Aoki[3], Takao M. Sato[2]

1.Planetary Plasma and Atmospheric Research Center, Graduate School of Science, Tohoku University, 2.JAXA, ISAS, 3.Istituto di Astrofisica e Planetologia Spaziali, INAF, 4.Graduate School of Science, Tohoku University, 5.College of Sicence, Rikkyo University

We report the current design of near-infrared spectrometer for the MMX (Mars Moon eXploration) mission, and also discuss near- and mid-infrared spectroscopy for next generation space projects with advanced imaging technology. MMX spacecraft is scheduled to be launched in the early 2020s, orbits Phobos and Deimos, and returns samples from Phobos back to Earth in the late 2020s. Near-infrared spectroscopy is useful to understand the material distribution on Martian moons (e.g., hydroxide minerals at 2.7 –2.8 um, hydrated minerals at 3.0 –3.2 um, and organics at 3.4 –3.4 um) and dynamics in Martian atmosphere (e.g. H2O at 2.5 –2.65 um, and pressure with CO2 absorption at 1.2 –2.2 um). We proposed a near-infrared spectrometer NIRS4 for the MMX mission to carry out the near-infrared spectroscopic measurement of the Martian moons Phobos and Deimos and Martian atmosphere. NIRS4 is based on the NIRS3 on the Hayabusa-2 spacecraft, which has a fast optics (F-number 1.4) with a long slit corresponds to a wide field-of-view (FOV) of 14.6 x 0.03 deg. NIRS4 covers the target area of 26 km length with 100 m spatial resolution looking from 100 km altitude. It also achieves 20 m and 1 m spatial resolution, respectively, from altitudes of 20 km and 1km. A grism is put in the collimating optics, and its wavelength resolution is ~ 1.5 to 3 nm (R~650 to 1000). A 2D HgCdTe array (640 x 512 pixel, pixel size 15 x 15 microns, sensitivity range 1 –3.8 microns) is used as a detector. The detector and optical system are cooled down below 90 K and 190 K with a Stirling cooler to reduce thermal noise. As an order sorter of dispersion light, we put 1– 1.9 um (1^{st} order) filter on a half part of the slit, and 1.9 –3.8 um (2^{nd} order) filter on the other half of the slit. In this way, a half FOV (7.3 x 0.03 deg) with wavelength range of 1 –1.9 um is focused on a half side of 2D detector (640 x 256 pixel area), and the other half FOV with wavelength of 1.9 –3.8 um is focused on the other half of the detector. The calibration lamp is used to determine the absolute wavelength. An optical chopping system which periodically interrupts an incident light to determine the background level precisely and to gain the signal-to-noise ratio.

Keywords: Mars, MMX, near-infrared spectrometer

Deployable Camera system 5 (DCAM5) proposed for Martian Moon Exploration mission (MMX)

*Koji Wada[1], Hirotaka Sawada[2], Kazunori Ogawa[3], Kei Shirai[2], Naoya Sakatani[2], Ko Ishibashi[1], Rie Honda[4], Minami Yasui[3], Masahiko Arakawa[3]

1.Planetary Exploration Research Center, Chiba Institute of Technology, 2.ISAS/JAXA, 3.Kobe Univ., 4.Kochi Univ.

We propose Deployable Camera system 5 (DCAM5) for remote and in situ observations of Phobos and Diemos in Martian Moon Exploration mission (MMX) led by JAXA. DCAM5 is the latest version of the DCAM series in space missions (DCAM1 and 2 were successfully operated in IKAROS mission and DCAM3 is equipped on Hayabusa2 mission). In this mission MMX, DCAM, a small handy-sized body equipped with several visible cameras, a triaxial accelerometer, batteries, and a communication unit will be separated from the spacecraft (SC) and thrown toward scientifically valuable regions of Phobos and Diemos where SC cannot approach nor land on, e.g., inner wall of Stickney crater.

As falling toward a target region, DCAM will take multiscale, multiband images of the target regions with a multiband camera equipped on the leading edge of DCAM. Multiband images with high resolutions down to ~ 1 cm/pix will reveal spectroscopic characteristics of the target region, such as the distribution of hydrated minerals and the texture of boulders which could reflect the thermal evolution of Phobos and Deimos. When DCAM collides to Phobos surface, we will measure the acceleration profiles at collision as an indicator of the mechanical properties of the landing point. From the acceleration profiles we will obtain the following properties depending on the nature of the landing point: (1) in the case of landing on a boulder, disruptive strength of boulders, which allows us to estimate Q* value reflecting the thermal evolution of Phobos, (2) in the case of landing on a regolith layer, penetration resistance (drag coefficient) of regolith layers which allow us to constrain the surface evolution inherent to Martian moons, and (3) in the case of a fine powder layer, compression curves of powder layers which reflects the porosity and the cohesion of the layer, constraining the levitation process on small bodies and the compression evolution of fluffly bodies such as planetesimals. After landing of DCAM, we will take close-up images of the surface to clarify the size and the porosity of the surface regolith.

Since DCAM is a light and small body, several DCAMs are preferred to be equipped and thrown toward different, valuable regions to reveal the origin and the evolution of Phobos and Deimos. Furthermore, we propose two objectives of DCAM5 other than the described above: one is to investigate candidate landing points on Phobos before landing of SC and the other is to observe the status of SC at around its landing and the disturbance of the landing points. Since each objective is achieved with one or more DCAMs, we need 3 DCAMs at least in order to complete all the objectives.

Keywords: Martian moons, planetary exploration, onboard instrument , DCAM

Geophysical experiments on Phobos proposed for JAXA Mars Moon Exploration mission

*Kazunori Ogawa[1], Satoshi Tanaka[2], Naoya Sakatani[2], Munetaka Ueno[1,2], Takeshi Hoshino[2], Kazutoshi Sakamoto[2], Taichi Kawamura[3], Yoshiaki Ishihara[2], Nozomu Takeuchi[4], Philippe Lognonné[3], Akito Araya[4], Ryuhei Yamada[5], Takeshi Tsuji[6], Taizo Kobayashi[7], Kei Shirai[8], Matthias Grott[9], Jerzy Grygorczuk[10], Axel Hagermann[11], Jörg Knollenberg[9], Tilman Spohn[9], Hideaki Miyamoto[4], Hiroaki Katsuragi[12], Sin-iti Shirono[12], Tomokatsu Morota[12], Masahiko Arakawa[1]

1.Kobe University, 2.Japan Aerospace Exploration Agency, 3.Institut de Physique du Globe de Paris, 4.University of Tokyo, 5.National Astronomical Observatory of Japan, 6.Kyushu University, 7.University of Fukui, 8.The Graduate University for Advanced Studies, 9.German Aerospace Center, 10.Polish Academy of Sciences, 11.Open University, 12.Nagoya University

Scientific instruments and their support devices are being proposed for geophysical experiments on Phobos as potential instruments for the Mars Moon Exploration mission (MMX). JAXA is currently planning a sample return mission to the martian moons. The spacecraft will stay in a quasi-orbit around Phobos for months or 1-2 years, and make scientific observations including remote sensing, landings on Phobos for sampling, and several flybys of Deimos. Scientific goals of MMX were defined as in the following two categories: (1) To reveal the origin of the Mars moons, and then to make a progress in our understanding of planetary system formation and of primordial material transport around the border between the inner- and the outer-part of the early solar system. (2) To observe processes that have impact on the evolution of the Mars system from the new vantage point and to advance our understanding of Mars surface environment transition. While a landing site for sampling is still under consideration, in a current plan the main spacecraft lands twice, on the “red” and “blue” areas on Phobos for example.
We proposed five scientific instruments for this mission. SEIS: a three-axes short-period seismometer and an active seismic vibration source, SSXT: a penetration probe of several tens cm length with temperature and thermal conductivity sensors, miniRAD: a miniaturized thermal infrared radiometer, a muon detector, and SUMIRE: a mechanical insertion resistance probe of 5 cm length. All these instruments basically aim at investigating the geophysical properties of the surface, sub-surface, and interior of Phobos, and their combined observations can provide integrated models of mechanical and thermal properties of the subsurface which has not been studied so far. The scientific objectives of these instruments are connected to the following mission objectives corresponding to the mission goals above: (a) To obtain indirect information on the Phobos internal structure in order to constrain the origin of Phobos independent of the sample analysis results. (b) To characterize the space environment and the surface features of Phobos, with the intention of comparison with asteroids.
Because the first four of the above scientific instruments require a long observation time at a fixed location, a long-lived landing package (MSM) is also proposed. SUMIRE is planned to be mounted on the feet of the mothership (main lander). Objectives of MSM are providing electric power, command/telemetry interfaces, and an operable environment for the scientific instruments throughout a period of our observations over a Mars year. MSM has the following specifications and functions: (i) Operates independently from the mothership and survives at a fixed point of area. (ii) Controls internal temperature in an operable range of the scientific instruments for their continuous observations. (iii) Provides wired interfaces of telemetry/command and power to the scientific instruments. (iv) Communicates over a radio link with the mothership in orbits and with ground-based stations on the Earth. MSM will be placed on Phobos’ surface during the landing sequence of the main spacecraft, and stay there over its entire lifetime.

Keywords: MMX, Martian moon, Phobos, Planetary exploration, Internal structure

Moments of inertia of Phobos with inhomogeneous internal structure

*Koji Matsumoto[1], Hitoshi Ikeda[2]

1.RISE Project Office, National Astronomical Observatory, 2.RDD/JAXA

The origin of Phobos is still an open issue. It may be either captured asteroid or formed from a disk of impact ejecta produced by a giant impact. Although it is not straightforward to determine the origin from internal structure alone, it will place important constraints. One of the key parameters related to the internal structure is moments of inertia (MOI). Phobos's MOI can be determined from amplitude of short-period forced libration and degree 2 gravity coefficients. Currently, the libration amplitude is estimated to be 1.09+/-0.01 degrees by analyzing multiple image data [1]. Although the degree 2 gravity coefficients are estimated from tracking data of Mars Express on its close flyby at Phobos, they are not solved for at sufficient accuracy [2]. Axial difference of MOI can be constrained by the libration amplitude, but currently MOI of Phobos is not known. The observed libration amplitude is consistent with homogenous mass distribution of Phobos, but local mass anomalies cannot be ruled out [1, 3]. Here we consider relatively simple two-layer internal structure and assume that ice water or porosity is confined in either layer, and calculate how much MOI deviate from the value for homogeneous body if such an inhomogeneity existed.
Phobos's bulk density of 1.86+/-0.013 g/cm^3 [4] is lower than most of the samples of carbonaceous material, which requires porosity and/or light elements like water ice. If the low bulk density was explained by water ice, its mass fraction is expected to be 10-35% depending on rocky material grain density [5]. If the mass distribution inside Phobos was inhomogeneous, e.g., water ice was concentrated near the surface or the center, we will observe a deviation of MOI from the value for homogenous interior. Here the MOI differences (dMOI) with respect to the homogenous Phobos are calculated for some cases where we assumed that (1) Phobos has a tri-axial ellipsoidal figure (a = 13.03 km, b = 11.40 km, c = 9.14 km), (2) Phobos has a two-layer structure and their boundary also has the similar ellipsoidal figure for which the libration amplitude is 1.15 degrees being consistent with the observed value of [1], and (3) water ice is confined either of the upper or lower layer and rock density is the same for both the layers. The water ice mass fraction is changed between 0 and 30% .
In the case that upper layer is composed of the rock plus water ice, when the upper layer thickness is 10% of the semi-principal axes, no more than 14 wt.% of water can be contained in the layer and the maximum dMOI is about 9%. When the layer boundary is deeper, more water can be contained, but the maximum dMOI is about 16%. In the case that the water ice is confined in the lower layer, the maximum dMOI is also about 17%.
We also tested the cases in which the porosity is responsible for the low bulk density. We calculated due to inhomogeneous distribution of the porosity using the similar two-layer structure. The results depend on the boundary depth and rock density. In the case that the lower layer is porous, the maximum dMOI is about 17% when rock density is 2400 kg/m^3, and about 9% when rock density is 2100 kg/m^3.
It is found that, for the layer configuration assumed here, dMOI is smaller than 16-17%. A 10% accuracy will not be sufficient, and it is required to achieve at least a few percent of MOI accuracy in order to detect it. To this end, the required accuracies for the libration amplitude and the degree 2 gravity coefficients are also a few percent.
References:
[1] Oberst et al. (2014) P*lanet. Space Sci.*, *102*, 45-50.
[2] Pätzold et al. (2014) *Icarus*, *229*, 92-98.

[3] Rambaux et al. (2012) *Astron. Astrophys.*, *548*, A14.
[4] Willner et al. (2014) P*lanet. Space Sci.*, *102*, 51-59.
[5] Rosenblatt (2011) *Astron. Astrophys. Rev.*, *19* (44).

Keywords: Phobos, internal structure , moments of inertia

Topographic degradation of craters on the moon of Mars, Phobos

*Seiya Morita[1], Tomokatsu Morota[1], Sei-ichiro Watanabe[1]

1.Graduate School of Environmental Studies, Nagoya University

The origin of the two Mars satellites Phobos and Deimos is controversial and evolution thereafter is also unclear. A numerical study showed that nearly all impact fragments ejected from the inner moon Phobos remain trapped in Mars orbits until re-impact with Phobos and produce new generations of ejecta. The suggesting process seems consistent with the observed thick regolith of Phobos. Such re-accumulation may also affect the shape of craters on Phobos. Thus, the crater morphology is expected to give us a key to read out the geological history of this enigmatic satellite. Contrary to rimmed craters on the Moon, craters on the low-gravity satellite Phobos have no clear rims, so that a new method of crater morphology applicable to low-gravity satellites should be developed.
On the Moon, the degradation of craters is controlled by the accumlation of smaller later impacts and follows topographic diffusion process. However, old lunar craters tend to be inconsistent with topographic diffusion model because ejecta deposits of larger later impacts effect crater degradation. On the Phobos, on the other hand, the crater degradation is expected to be consistent with topographic diffusion model in the longer time scale than that on the Moon because impact fragments spread all over the Phobos surface and large later impacts have a smaller effect on the shape of craters than the Moon.
So, I propose a crater shape analysis based on a topographic diffusion model, applicable to craters on a small body, and estimate the model ages of Phobos craters from the degree of crater degradation. I made averaged topographic profiles of twenty craters with radii larger than 1km and compared each of them with a diffusion-model profile having the same flection-point radius.
I find that the topographic profiles of most of the craters are consistent with corresponding diffusion profiles. Further, in each crater, the maximum angle of slope is proportional to depth normalized by the flection-point radius, which is consistent with the prediction of the topographic diffusion model, and the model age kt (where k is the topographic diffusivity and t is the crater age) can be determined. The distribution of kt of the craters is, however, concentrated in lower values, which is inconsistent with the topographic diffusion model with k correlated to crater-forming impact flux. These results suggest that Phobos experienced some unique erosion process incompatible with simple topographic diffusion models.

Keywords: Phobos, crater, degradation

Geological investigation of the blue unit on Phobos

*Hiroshi Kikuchi[1], Hideaki Miyamoto[1], Ryodo Hemmi[1]

1.The University Museum,The University of Tokyo

The surface of the Martian satellite, Phobos, is spectrally divided into two units: red and blue. Understanding their difference may be key to determining the origin and evolution of Phobos, because the blue unit has commonly been interpreted to be composed of original materials of Phobos. Whereas the red unit is distributed nearly globally, the blue unit maps to some relatively small impact craters and the largest crater on Phobos, ~ 9 km-diameter Stickney crater, and its nearby surroundings. Hypotheses to explain its distribution include: (1) emplacement of low-velocity ejecta from the Stickney impact [1], (2) landslide materials extending to the west of Stickney crater [2], and (3) an inner heterogeneous structure of Phobos [e.g., 3; 4]. Regarding (1), Thomas 1998 suggests that low-velocity Stickney ejecta are capable of distributing asymmetrically due to the effects of Phobos' rapid spin, however the emplacement velocity did not be considered. The ejecta may have been emplaced beyond the extent hypothesized. Using high-resolution images, we investigate this with high precision.
We examine the largest region of the blue unit east of Stickney by: changing the NIR/BG color ratio for the western part of HiRISE (High Resolution Imaging Science Experiment) images based on the analysis of [5]. In order to compare these maps, we create a dynamical potential map by dividing the numerical shape model [6] into 1,672,215 small triangular pyramid. From the tidal, centrifugal, and self-gravitational forces [7], we calculate the dynamical potentials at 121,770 points on the surface of Phobos. In addition, we perform numerical simulations in order to examine the relationships between the patterns of Stickney ejecta and regions of blue unit. Considering the rotation of Phobos, as well as the gravity of Phobos and Mars, we map the emplacement where the simulated orbit of particles and the sphere of Phobos intersect and calculate the emplacement velocities based on our simulations. In the calculation of the potentials and the simulations, we change values of the distance between Phobos and Mars from 20,000 km to 9,376 km to account for the changing distance through time. Moreover, we calculate the angle and the direction of the potentials.
As a result, many blue materials exist on the floor of craters and grooves. Comparing the spatial extent of the blue unit in the region east of Stickney crater to the slope map, a greater occurrence of the blue unit is observed on gentle slopes with increasingly less occurrence with greater slope angle. When performing comparative analysis among the maps generated based on varying orbital distances, the extent of the blue unit appears to be consistent with the current orbit. From our simulations, the emplacements of low velocity ejecta of Stickney cover one of blue unit regions east of Stickney.
Our results suggest that blue material easy to move rather than red material. Moreover if the origin of materials composing the blue unit is ejecta of an impact crater of Phobos, the emplacement velocity of the ejecta deposits must be lower than the escape velocity of Phobos. Based on these investigations, we interpret that the Stickney crater is underpinned by the blue unit with its surface being modified into the ubiquitous red unit through space weathering among other processes. Subsequently, the impact event except for Stickney might expose fresh blue materials.
[1] Thomas P. C. (1998) *Icarus, 131*, 78-106. [2] Shingareva T. V. and Kuzmin R. O. (2001) *Sol. Syst. Res, 35*, 431-443. [3] Murchie S. et al. (1991) *JGR, 96*, 5925-5945. [4] Basilevsky A. T. et al. (2014) *PSS, 102*, 95-118. [5] Thomas N. et al. (2011) *PSS, 59*, 1281-1292. [6] Gaskell R.W. (2011) Gaskell Phobos Shape Model V1.0. VO1-SA-VISA/VISB-5-PHOBOSSHAPE-V1.0. NASA Planetary Data

System. [7] Thomas P. C. (1993) *Icarus, 105*, 326-344.

Keywords: Phobos, Blue unit, Stickney crater

Solids and Fluids of volatile (carbon)-bearing materials on Asteroids and Martian Moons

*Yasunori Miura[1]

1.Visiting (Yamaguchi, In & Out Universities)

Introduction
Asteroids and Moons (of Earth and Mars) are studied mainly from material sciences of mineral and texture with formation ages by using database of Earth' rocks and collected meteorites (Asteroids and Earth's Moon), where the collected meteorites show quenched texture and limited mineral-solids without remained fluids. The main purposes of the paper is to elucidate formation processes of solids and fluids of Asteroids and the Moons.
Solidified fluids on meteorites:
Remained fluid-water cannot be obtained at meteorites and Moon (Earth) rocks, because global water (on Earth) with formation of many mineral series and rock kinds cannot be confirmed. Fluid formation of these meteorites are rapidly solidified to be formed groundmass among chondrules and/or phenocryst of crystalline minerals. This indicates that fluids are formed quickly and changed to non-crystalline aggregates to fix solids of chondrule crystalline grains from meteorite texture.
Solidified micro-grains produced by laser melting:
Author has produced quick fluids texture during laser sputtering experiments of carbon-bearing rocky grains in this study. This indicates formation of fluid liquid phase from solid mineral to quenched grains though there are no previous fluid water in the sample before laser sputtering process..
Similar heating experiment of carbonaceous meteorite produces only water after heating reaction though there are no water before heating.
The present experimental results indicate that there are any elements, ion and elements of fluids (water and carbon dioxides) are existed separately and combined by extreme conditions of high temperature and pressure, which can explain clearly the poor mineral and rock kinds compared with water-planet showing circulated fluids and water supply by interior activity.
Carbon-bearing materials formed at collisions on asteroids.
Almost all evaporated elements are disappeared without any remained solidified materials (except carbon-bearing grains) after impacted collision on Asteroid surface. In fact, we can observed solidified carbon-bearing nano-grains on the Moon rocks (Africa and Antarctica) and chondritic meteorites (ordinary to carbonaceous samples), which indicate that the Moons and any Asteroids have volatile carbon-bearing materials on the surfaces.
Expected space explorations for the Moons and Asteroids:
Among many Asteroids, volatile (carbon)-bearing materials are produced for active multiple collisions (including impact crater sites) or largely broken small bodies by huge collision, where many material resources with volatiles (carbon and/or hydrogen) are expected to be find for next human resources on space world in future.
Summary:
Natural resources of volatile (carbon)-bearing materials on the two Moons (Mars) and Asteroids are expected for next target for sample collection and material circulation sites for limited living bases in future, which are obtained by meteorite analyses and artificial laser experiments.

Keywords: Solids and Fluids , Volatile (carbon)-bearing materials , Asteroids and Martian Moons

Gravity science investigation of Ceres from Dawn

*Ryan Park[1]

1.Jet Propulsion Laboratory, California Institute of Technology, Pasadena, CA, USA, 2.IMCCE, Observatoire de Paris, Paris, France, 3.Massachusetts Institute of Technology, Cambridge, MA, USA, 4.Lamont-Doherty Earth Observatory, Columbia University, Palisades, NY, USA, 5.University of Toulouse, Toulouse, France, 6.UCLA, Los Angeles, CA, USA.

R.S. Park[1], A.S. Konopliv[1], B.G. Bills[1], N. Rambaux[2], J.C. Castillo-Rogez[1], C.A. Raymond[1], A.T. Vaughan[1], A. Ermakov[3], M.T. Zuber[3], R. Fu[4], M.J. Toplis[5], C.T. Russell[6], [1]Jet Propulsion Laboratory, California Institute of Technology, Pasadena, CA, USA (e-mail Ryan.S.Park@jpl.nasa.gov); [2]IMCCE, Observatoire de Paris, Paris, France; [3]Massachusetts Institute of Technology, Cambridge, MA, USA; [4] Lamont-Doherty Earth Observatory, Columbia University, Palisades, NY, USA; [5]University of Toulouse, Toulouse, France; [6]UCLA, Los Angeles, CA, USA.

The Dawn gravity science investigation utilizes the DSN radiometric tracking of the spacecraft and on-board framing camera images to determine the global shape and gravity field of Ceres. The gravity science data collected during Approach, Survey, and High-Altitude Mapping Orbit phases were processed. Currently, the latest gravity field called CERES08A is available, which is globally accurate to degree and order 5. Combining the gravity and shape data gives the bulk density of 2163+-8 kg/m^3. The low Bouguer gravity at high topography area, or vice versa, indicates that the surface of Ceres is likely compensated and that its interior presents a low-viscosity layer at depth. The degree 2 gravity harmonics show that the rotation of Ceres is very nearly about a principal axis. This is consistent with hydrostatic equilibrium at the 3% level. This infers that the mean moment of inertia of Ceres is , implying some degree of central condensation. Based on a simple two-layer model of Ceres and assuming carbonaceous chondrites and hydrostatic equilibrium, the core size is expected to be ~280 km with corresponding average thickness of the outer shell of ~190 km and density of ~1950 kg/m^3.

Keywords: Ceres, Dawn, Dwarf planet

The Instrument error on estimation of normal albedo of Ryugu using the laser altimeter on-board Hayabusa2 and the reflectance measurement of the carbonaceous chondrite at zero phase angle

*Ryuhei Yamada[1], Hiroki Senshu[2], Noriyuki Namiki[1], Takahide Mizuno[3], Shinsuke Abe[4], Fumi Yoshida[1], Kazuyoshi Asari[1], Hirotomo Noda[1], Naru Hirata[5], Shoko Oshigami[1], Hiroshi Araki[1], Yoshiaki Ishihara[3], Koji Matsumoto[1]

1.National Astronomical Observatory of Japan, 2.Chiba Institute of Technology, 3.Japan Aerospace Exploration Agency, 4.Nihon University, 5.The University of Aizu

The Japanese asteroid explorer ‘Hayabusa2’ was launched at end of 2014 to explore the near-Earth C-type asteroid ‘Ryugu’. In this mission, we have a plan to apply the laser altimeter (LIDAR) on-board Hayabusa2 to investigate the distribution of normal albedo of Ryugu at a laser wavelength (1064 nm). The LIDAR instrument for laser ranging which has a function to measure the intensities of transmitted and received pulses. The intensities data can be used to estimate the normal albedo of Ryugu.

In this study, we evaluated the contribution of the instrument error to the normal albedo uncertainty on the estimation from the intensities data. From the evaluation, we found the error due to instrument effects was 18% at an altitude of 20 km based on the verification tests of the LIDAR flight model. The surface slope and roughness elongate the time width of the returned pulse and decrease the intensity. We will also describe how the returned pulse is deformed as a result of slope and roughness.

Currently, we prepare for reflectance measurment of the carbonaceous chondrites at observation condition of the LIDAR to obtain calibration data to interpret the normal albedo variation on Ryugu. In this experiment, we enabled measurement of the reflectance at zero phase angle and wavelength of 1064 nm using a beam splitter. Then, to compare and integrate the normal albedo estimated from the LIDAR data with the reflectance data measured by other instrument equipped on Hayabusa2 (the optical camera and near-infrared spectrometer), the phase angles can be controlled from 0 to 30 degrees on the experiment. In this presentation, we will report configuration of the reflectance measurement and preliminary results.

Keywords: Asteroid albedo, Ryugu, Hayabusa2, Laser altimeter, Carbonaceous chondrite, Refelectance measurement

The origin of Itokawa dimples and a comparison with the surface structure of Phobos

*Masato Kiuchi[1], Akiko Nakamura[1]

1.Graduate School of Science, Kobe University

High-resolution images of asteroid 25143 Itokawa obtained by Hayabusa mission revealed that the surface of Itokawa has unique feature compared to other asteroids. The surface of Itokawa can be divided into two regions, one is rough terrain composed by many boulders and the other is smooth terrain composed by fine materials. On the smooth terrains small dimples associated with boulders are observed. This structure was considered as results of low-velocity impacts of boulders (Nakamura et al., 2008) or seismic shaking beneath boulders (Hirata et al., 2009), however, the origin of dimples have not been understood.
Although widely used successfully for craters on planetary surfaces, whether the scaling law about crater size (Holsapple, 1993) can be applied to low-velocity impacts is not obvious. This scaling law was originally derived based on point source approximation which can be applied when the crater size is sufficiently large as compared with impactor size. Moreover, the gravity dependence of crater diameter has not been fully understood. Hypervelocity impact experiments were conducted under increased gravities (Schmidt and Housen, 1987) and under low gravities (Gault and Wedekind, 1977). In these experiments crater diameter was proportional to about -0.17 power of gravitational acceleration. However, there are few impact experiments under different gravity condition except above experiments.
We developed a drop mechanism which can simulate gravities smaller than 1 G. A target container was suspended by springs of constant force, or fallen freely to archive simulated gravity range between 0.01 and 1 G. We used silica sand of average diameter 140 μm as the target material. Stainless steel sphere of 8 mm diameter was impacted onto the target and the impact velocity was between 1 and 5 ms^{-1}. As a result, the crater diameter was proportional to -0.19 ±0.01 power of the gravitational acceleration. This value is roughly in agreement with previous studies at hypervelocity (Kiuchi and Nakamura, 2015 JPGU meeting).
However, the crater diameter obtained by our experiments is not on the line expected from the scaling law (Holsapple, 1993) as shown in the Figure. This difference is caused by a difference of the power-law exponents of π_2; the exponent is -0.19 for low-velocity impacts and -0.17 for hyper-velocity impacts. A steeper exponent, -0.25, was obtained for our new impact experiments with glass bead projectiles conducted in the similar setup. These results suggest that the impact energy is consumed for crater formation more efficiently at low-velocity impacts compared to hypervelocity impacts.
We estimated the crater diameter formed by re-impacts of boulders ejected from primary crater on Itokawa based on results of our experiments. We assumed that these boulders impact onto smooth terrain at escape velocity of Itokawa, 0.17 ms^{-1}. By combining with these conditions of Itokawa surface and the scaling law obtained by our low-velocity impact experiments, the crater diameter formed by the impact of a boulder of diameter 2 m would be 7 -8 m. Note that the impact velocity assumed was the maximum value and the effect of porosity difference between the laboratory and Itokawa surface was not considered here, however, the estimated crater diameter was consistent with observational data in which the diameter of dimple associated with a boulder of diameter 2m is about 7 m. This result supports the possible low-velocity boulder-impact origin of dimples.
We applied similar estimate to boulders derived from Stickney crater of Phobos. As a result, craters which have about 2 to 3 times diameter of boulders would be formed. However, we have not identified dimples associated with boulders on surface images of Phobos. This may be due to a

difference of the surface structure of Itokawa and Phobos and/or due to a difference of surface evolution processes of two bodies.

Keywords: dimple, Itokawa, impact experiments, Phobos

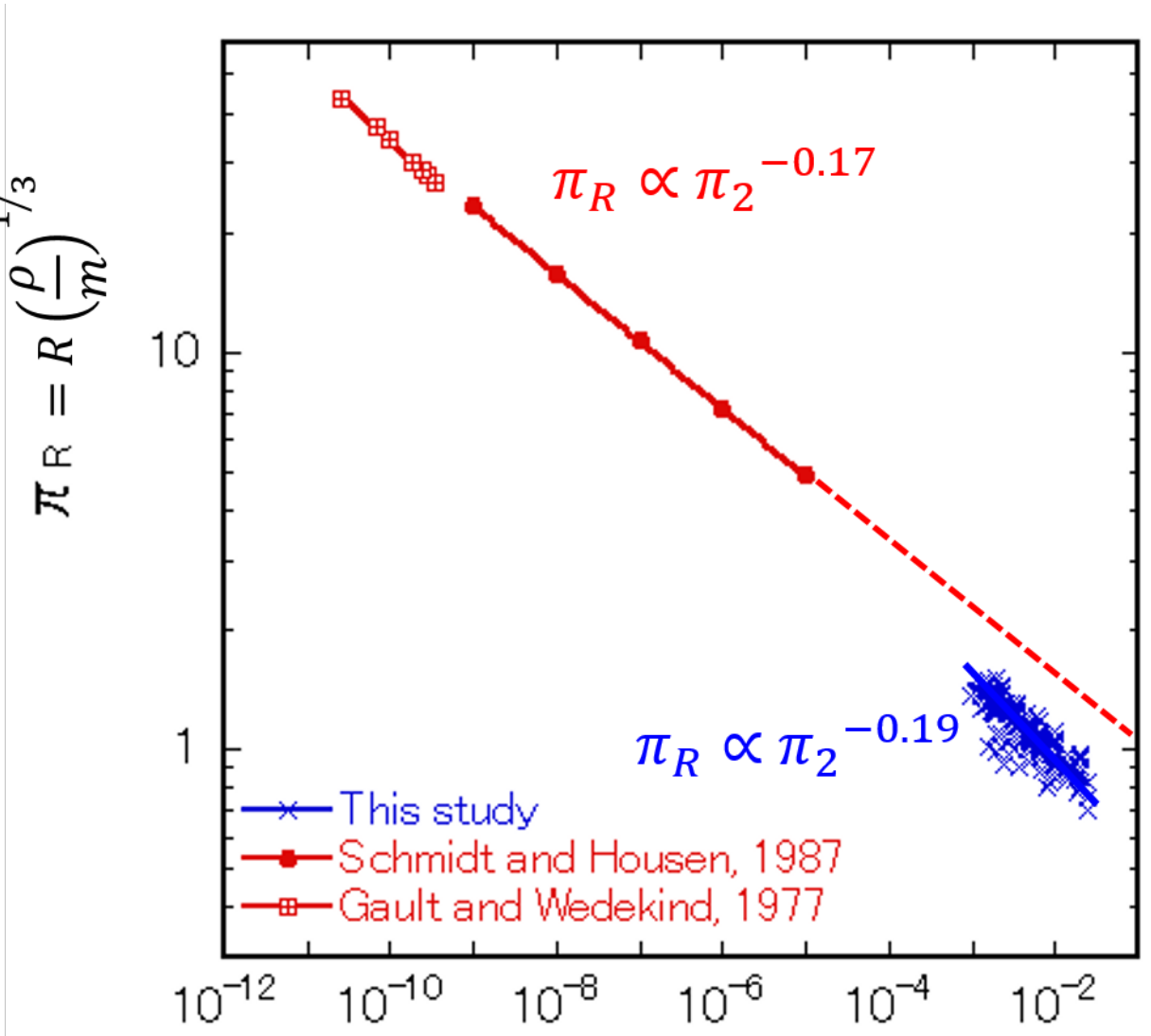

g: gravitational acceleration
a: impactor radius
v: impact velocity, R: crater radius
ρ: target density, m: impactor mass

$$\pi_2 = \frac{ga}{v^2}$$

Earth-moon images captured by Hayabusa2 visible cameras during Earth swing-by

*Seiji Sugita[1], Manabu Yamada[2], Hirotaka Sawada[3], Tomokatsu Morota[4], Rie Honda[5], Shingo Kameda[6], Chikatoshi Honda[7], Hidehiko Suzuki[8], Toru Kouyama[9], Kazunori Ogawa[10], MASATERU ISHIGURO[11]

1.the University of Tokyo, 2.Chiba Institute of Technology, 3.JAXA, 4.Nagoya University, 5.Kochi University, 6.Rikkyo University, 7.Aizu University, 8.Meiji University, 9.AIST, 10.Kobe University, 11.Seoul National University

JAXA's Hayabusa2 completed an Earth swing-by on December 3th of 2015. During this opportunity, we photographed both Earth and Moon with three optical navigation cameras (ONC-T, W1 and W2). Since this was the last opportunity to observe extended light source before reaching the target asteroid Ryugu, the obtained images are extremely important for calibration of our cameras. In this paper, we present the Earth-Moon images and preliminary analysis results.

Phase angle dependency on reflectance spectra and ultraviolet spectroscopy of carbonaceous chondrites.

*Tomohiro Takamatsu[1], Shingo Kameda[1], Seiji Sugita[2]

1.School of Science, Rikkyo university, 2.Department of Earth and Planetary Science, Graduate School of Science Science, The University of Tokyo

The Hayabusa2 spacecraft was launched in 2014, and is expected to arrive at the asteroid Ryugu, which belongs to the C-type asteroids. One of the objectives of the Hayabusa2 mission is to return primordial samples that do not show advanced thermal metamorphism. Vilas (2008) used reflectance spectroscopy from the ground to determine that Ryugu has absorption of approximately 700 nm, indicating the presence of hydrated minerals. The Hayabusa2 spacecraft performs multi-band spectrum observation using ONC-T, which is a telescopic optical navigation camera with seven band-pass filters, and specifies the spot at which the 700 nm absorption feature exists for landing. Therefore, it is important to confirm the detectability of the absorption of 700 nm from multi-band spectral observation. We performed multi-band spectral imaging of carbonaceous chondrites that indicate the same reflectance spectrum as C-type asteroids by using the ONC-T flight model and detected the 700 nm absorption feature at a phase angle of 30° for light-source-sample-ONC-T (Kameda et al, 2015). On the contrary, the phase angle of sun-Ryugu-Hayabusa2 is expected to vary in the range from 0°-40°, while the Hayabusa2 spacecraft is in the vicinity of Ryugu. Therefore, it is also necessary to confirm the detectability of the 700 nm absorption feature in the phase angle of 0°-40° from multi-band spectral observation.

In this study, we perform reflectance spectroscopy of these carbonaceous chondrites using a camera that imitates ONC-T to detect the 700 nm absorption feature in the phase angle range of 0°-40°.

We construct an experimental system in which the incidence angle is variable in the range of 0°-40°and the emission angle is fixed by using a half mirror and a rotation stage. We measure the reflectance spectra and depth of the 700 nm absorption feature of the carbonaceous chondrites using a camera having the same CCD and bandpass filters with nearly identical center wavelengths as that of ONC-T. In this presentation, we report a result.

Moreover, this paper discusses the progress of an investigation about identification of satellite surface materials by ultraviolet observation for a Mars satellite exploration project planned for launch in 2022.

Keywords: Small Solar System Bodies, Multi-band imaging, carbonaceous chondrite

Effect of iron sulfide on the space weathering of asteroids

Mizuki Okazaki[1], *Sho Sasaki[1], Takahiro HIroi[2], Toru Matsumoto[3], Akira Tsuchiyama[4], Akira Miyake[4], Takafumi Hirata[3,4]

1.Department of Earth and Space Sciences, School of Science, Osaka University, 2.Department of Earth, Environmental, and Planetary Sciences, 3.ISAS/JAXA, 4.Department of Earth and Planetary Science, Kyoto University

The space weathering alters surface optical properties on airless bodies such and asteroids, the Moon and Mercury. As for silicate bodies containing iron silicate, the space weathering (characterized by optical reddening, darkening and attenuation of Fe-related absorption) is caused by nanophase metallic iron (npFe^0) particles within vapor-deposited amorphous rim by micrometeorite impacts or within amorphous rim by solar wind implantation.
However nanophase iron sulfide (npFeS) was found in Itokawa particle's space weathered rim (Noguchi et al., 2011) and was observed more frequently than npFe^0 in regolith breccia meteorites (Noble et al., 2011). Therefore we performed experiments of pulse laser irradiation to olivine and FeS mixture samples to explain the effect of FeS on space weathering. The samples which 5, 10, 20 weight % FeS mixed to olivine of particle size 45-75 micron was made and irradiated at 10 mJ once or twice. Some of laser irradiated samples were also conducted additional thermal fatigue experiments. After laser irradiation and/or thermal fatigue experiments, reflectance spectra of samples were measured, and some of laser irradiation samples were observed by microscopes; FE-SEM, HRM, TEM and SEM-EDS.
The results show FeS promote vapor deposition type space weathering, especially overall darkening. The spectra of samples including FeS showed more reddening and also overall darkening, and also fine FeS particles are highly effective. Thermal fatigue experiments after laser irradiation show that darkening was back to standard but reddening remained. This results show that spectral change especially darkening is not stable against heating simulating asteroidal surface. Our HRM, TEM and SEM-EDS observation suggest npFeS particles exist but have not been exactly identified in this study.
Therefore, addition of FeS particles promote reddening by formatting npFe^0 on the surface of olivine particles. The cause of darkening is not micro-scale particles but macro-scale sulfur deposition by HRM, TEM and SEM-EDS observation. Thermal fatigue experiments in this study show sulfur can easily vaporize from surface, which suggests sulfur on asteroids is less than in meteorites.

Keywords: Space weathering, asteroids, sulfur, reflectance spectrum

High velocity impact experiments for frozen sands related to crater scaling laws in strength regime

Shota Takano[1], *Masahiko Arakawa[1], Minami Yasui[1], Kazuma Matsue[1], Sunao Hasegawa[2]

1.Graduate School of Science, Kobe University, 2.Japan Aerospace Exploration Agency

Solid bodies in the outer solar system are mostly covered with icy crust, and it is composed of ice-rock granular mixture. There are a lot of impact carter on these surfaces, and crater scaling laws are necessary to derive information of impacted bodies from the observed craters and to estimate the regolith thickness deposited on the surface from the ejected material. Especially, on middle and small icy bodies, the crater formation process could be controlled by the material strength of the icy crust, so that the crater scaling laws applicable to the strength regime is necessary to study the crater observed on these small and middle size icy bodies. However, the crater scaling law in the strength regime has not been confirmed by the experiments using the material continuously changing the strength; especially, the ejecta velocity distribution in the strength regime has no been studied yet so far. Therefore, we conducted the impact cratering experiments on the icy material with the various strength to elucidate the material strength dependence on the ejecta velocity distribution and the crater size.
We used frozen quartz sand targets with the water content from 2.5 to 20 wt.%, and they were made at -20 degrees using quartz grain with the size of 100mm. This frozen sample was tested to obtain the tensile strength (Y) changing with the water contents (C), and the empirical equation was derived as follows, Y(MPa)=0.145C (wt.%). The impact experiments were conducted at 2, 4 and 6km/s using an aluminum projectile with the diameter of 2mm, and the frozen target was impacted by the projectile on the surface normal to the impact direction.
As a results, the crater formed on the frozen sand with various strength was found to change with the mechanical strength and the crater size increased with the decrease of the strength. The pi-scaling theory for the crater size was applied to these results and the following equation was obtained: $\pi_R=1.0p_Y^{-0.3}$, where $\pi_R=R(\rho/m)^{1/3}$, $\pi_Y=Y/\rho v_i^2$, R: crater radius, ρ: target bulk density, m: projectile mass, and v_i: impact velocity. We also measured the ejecta velocity distribution, which was the relationship between the initial ejection position and the ejection angle or the ejection velocity. Then, the ejection angle was found to increase with the distance from the impact point and to become very steep until vertical near the crater rim, and this feature of the ejection angle changing with the distance could cause the unique ejecta curtain call a pillar, which was ejecta curtain extending normal to the target surface. The pillar-like ejecta curtain could be a unique one formed in the strength regime, and it might be originated from the restricted ejecta flow field inside the crater.

Keywords: solar system small bodies, high velocity impact , crater scaling law

The survey of physical properties of planetary subsurface using penetrator

*Masashi Okazaki[1], Masahiko Arakawa[1], Minami Yasui[1], Kazuma Matsue[1], Shota Takano[1]

1.Graduate School of Science, Kobe University

Physical properties of planetary surface such as porosity, grain size etc. are important features to control the thermal and mechanical properties of airless planetary surfaces, then the surfaces such as asteroids and the Moon have been observed by various remote sensing methods. However, the information obtained by the remote sensing is very limited on the mechanical properties of the subsurface layer. While the subsurface mechanical properties are important to elucidate the evolution of the surface geology induced by impacts and tectonics. Then, the exploration method has been studied for the subsurface investigation. A penetrometry is one of the candidates to investigate the subsurface mechanical properties in planetary explorations, and it has been already used for the Cassini-Huygens mission and was planned for Luna-A mission.

In this study, we studied the scientific aspect of the penetrometry, especially for the instrument called as a penetrator. The penetrator usually contains some instruments and can penetrate into planetary subsurface, then it can measure subsurface physical properties during the penetration. Particularly, we focused on the instrument of the accelerometer equipped on the penetrator, which can measure acceleration the resistance force induced from the subsurface materials.The resistance force acquired by the accelerometer on the penetrator would have information of the mechanical properties of the subsurface material. Then, in order to derive the information of the subsurface features from the resistance force, we should know the relationship between the resistance force and the physical properties of the granular layer simulating the subsurface regolith layer.

Therefore, we carried out penetration experiments on various regolith simulant in order to clarify the relationship between the resistance force and the physical properties of the regolith simulant. The resistance force was analyzed to construct the constitutive equation charactering the regolith simulant, and this equation could be useful to analyze the observation in the future mission and to study the evolution of the surface geology.

We used a cylindrical stainless penetrator with the diameter of 2.6cm and the height of 4.35cm. The accelerometer was mounted on the back side of the penetrator, and the penetrator was dropped at various heights to change the penetration velocity and free-fell on the target.We prepared the target by using spherical glass beads (0.5μm, 100μm, 200μm, 500μm, 1mm, 1cm), red clay (2-4mm), quartz sand (100μm, 500μm), and perlite (2-3mm). They were poured into an acrylic cubic case (15cm in each side).The penetrator was dropped through the acrylic cylinder with the inner diameter of 3 cm to control the position of the penetrator and to confirm the impact normal to the target surfaces.

In our experiment, the acquired wave forms showing the resistance forces were evaluated according to the following features: the maximum acceleration value, the acceleration value just before the penetration stop, the duration of the acquired wave. As a result, we found the relationship between the resistance force and the physical properties (porosity, granular size) and constructed the constitution equation for each regolith simulant, and then each equation could be used for the clue to identify the surface materials comparing with the observational data from the penetrator.

Keywords: penetrator, physical property, subsurface

54Cr Isotopic Anomalies in Asteroids Caused by Injection and Diffusion in Solar Nebula

*Taishi Nakamoto[1], Akira Takeishi[1]

1.Tokyo Institute of Technology

Temporal change of ^{54}Cr isotopic ratio in meteorites:
Chromium has four stable isotopes: their mass numbers are 50, 52, 53, and 54. The ratio of ^{54}Cr to the major isotope ^{52}Cr in various meteorites including chondrites, differentiated meteorites, and iron meteorites shows variations (anomalies). Sugiura and Fujiya (2014) estimated formation ages of each meteorite parent body and found that ages of meteorite parent bodies and the degree of ^{54}Cr isotopic anomalies in the meteorites are in a good correlation. They thought that this relation is caused by an increase of ^{54}Cr-rich particles contained in meteorites. Based on this interpretation, they carried out numerical simulations, in which small ^{54}Cr-rich dust particles are injected into the solar nebula at a certain time and diffuse in the nebula, and showed that the correlation can be reproduced by the small grain injection model.
Injection Model Revisited:
Although the Sugiura and Fujiya model is interesting and attractive, we think some points should be reconsidered. First, they assumed that small dust particles from a supernova arrive only at a narrow ring area on the disk at a certain distance from the central star. However, the injection to such a narrow ring seems unrealistic. Secondly, they supposed that the solar nebula is static. The solar nebula evolves in the time scale not much different from the time scale of parent body formation. Thus, we examine the concentration of ^{54}Cr-rich dust particles in the solar nebula as a function of time with a uniform injection model. The solar nebula dynamical evolution is also taken into consideration.
Results:
We obtained results that the concentration of ^{54}Cr-rich grains in the meteorite parent body formation region increases as the time. The surface density of the solar nebula decreases with radial distance, and we suppose that the material is injected uniformly, then after the injection, the concentration of ^{54}Cr-rich small grains per unit disk area becomes an increasing function of the radial distance. Since the meteorite parent body formation region is rather close to the Sun, e.g., 2 - 4 AU, the concentration in that region is initially low. On the other hand, diffusive motion of small grains in the solar nebula is caused by turbulence, and the mass flux due to the diffusion is in proportion to the gradient of the concentration. So, the distribution of concentration approaches a flat one with time. Thus, the concentration in the meteorite parent body formation region increases with time.
According to our numerical simulations, the quantitative relation between the ^{54}Cr anomalies and the parent body ages obtained by Sugiura and Fujiya (2014) can be reproduced when the turbulent diffusivity parameter a, which is a model parameter representing the strength of turbulence in the disk, is of the order of 10^{-3} - 10^{-2}.

Keywords: Isotopic Anomaly, Solar Nebula, 54Cr, Meteorite Parent Body Formation, Injection

4-D calculation of prediction of Perseid

*Isao Sato[1], Yushi Imamura[1], Shinsuke Abe[1]

1.Nihon University

Dust trail theory at present is under the hypothesis that meteoroids have been ejected at the perihelion of the orbit of the parent body of the meteors. However, the meteoroids colliding to the earth have been ejected not at the periherion but some point on the orbit of the parent body. We reveal that when and where the meteroids have been ejected on the orbit of the parent body with 3-D velocity vector.

Keywords: meteor, 4-D calculation, perseid

Possible duplicity of some asteroids discovered in Japan

*Isao Sato[1], hamanowa Hiromi, Tomioka Hiroyuki, Uehara Sadaharu, Tsuchikawa Akira

1.Nihon University

We present the possible duplicities of the asteroids (279)Thule, (324)Bamberga, (624)Hektor, (657)Gunlod, and (3220)Murayama which were discovered in Japan.

Keywords: asteroid , satellite

What can be obtained in Mult Impact Hypothesis by Abduction? Approaching the mystery of Origin of "Solar system and Asteroid belt"!

*Akira Taneko[1]

1.SEED SCIENCE Lab.

The origin of the moon and asteroids, remains unresolved.
There is a distance from the earth, a past of biological birth before, but further experiments impossible.
But can be elucidated in meteorite research, is a rare material available,
thermal history by burning at the time of fall is it difficult to origin analysis.
It can not be explained that there is a differentiated meteorites (Stony, iron, stone iron meteorite)
and undifferentiated meteorite.
What can be obtained in Mult Impact Hypothesis by Abduction?
Approaching the mystery of Origin of "Solar system and Asteroid belt"!
Efficacy of abduction is determined all in the selection of "physically meaningful hypothesis".
"That multiple conclusions can be explained systematically without contradiction to each other the current situation" is the proof.
The "Multi-Impact Hypothesis," to give the hypothesis with the following "Linking the moon and the earth of the Missing Link," a unified reasoning of (A) and (B).
(A) Differentiated protoplanetary CERRA of Mars size formed in the asteroid belt position of the solar system,by the perturbation of the most recent of Jupiter (giant mass), orbit is flattened to Jupiter near point side.
(B) Immediately before the CERRA to Jupiter collision, ruptured at a tension of Jupiter and the sun,the mantle piece collide intersects the Earth orbit.by Abduction
(1) Moon of origin: collision mantle piece to Earth (12.4km / s, 36.5 degrees), and formed in the orbit radius 60 · Re position
*(2)Pacific Rim arc-shaped archipelago marginal origin: In the Pacific Ocean position collision at the time of moon formation, Depression marginal sea forming in all directions
*(3)By a large amount of mantle deficient moon formation collision, Van Allen belt of Brazil of core eccentricity (about 10%) was reduced.
*(4)CERRA it takes about 5-6 million years until the track flat torn in Jupiter perturbation, had already differentiated cooling.
*(5)Multiple of mantle piece collide to Eartht by peeling off the mantle , 70% of the sea surface of the earth -5km was formed by isostasy.
*(6)Origin of plate tectonics PT , minimization of the eccentric and the moment of inertia caused by the collision as the driving force.
*(7))Origin of plate boundary , Crust peeling due to the mantle piece collision and crack formation
*(8)Origin of arc-shaped archipelago and Marginal basin plate : Mantle deficit by collision and plate concave formed by isostasy
*(9)The origin of the start of subduction convex plate : When the concave plate and the convex plate each other press by the driving force , cause the convex crawl under concave.
(10)Fragments at break of CERRA is the origin of the asteroid belt. Understood in the distribution of long radius (kinetic energy)
(11)The meteorite, but differentiated stony, stony-iron and iron meteorites are mixed , it can be understood with the fragments of CERRA.

(12)There are several fragments of CERRA, large species extinction repeated happened with sequentially collision.
(13)Core and part of the mantle of CERRA , the mass is large energy such as distribution, It became a low orbital energy Mercury with law of equipartition of energy.
(14)The fragments of CERRA that has collided to Jupiter, was the origin of the Great Red Spot.
cf. Shoemaker Levy No. 9 comet collide with Jupiter in July 1997, collision marks remained about half a year as small red spots.
If large Serra of debris from the comet, it is possible to maintain the Great Red Spot without disappear from the hundreds of millions of years ago. Is this in the finished demonstration experiment?
To estimate the origin of the asteroid belt, what to elucidation of purposes in the sample return plan is made clear.

Keywords: the mystery of Origin of " Asteroid belt", Abduction, Multi-Impact Hypothesis, The origin of Aasteroid, Origin of differentiated Meteorites, Undifferentiated Meteorite, Chondrite